QUENCHING OF THE WEAK AXIAL-VECTOR COUPLING STRENGTH IN β DECAYS*

Jouni Suhonen

University of Jyväskylä, Department of Physics
P.O. Box 35, 40014 Jyväskylä, Finland

(Received December 5, 2017)

The quenching of the weak axial-vector coupling strength, $g_{\rm A}$, in nuclear β decays is reviewed. The quenching is discussed for both the Gamow–Teller decays and the forbidden β decays of different variants. Both the historical background and the present status are reviewed and compared with each other. Possible new measurements are urged, whenever relevant for determining the amount of $g_{\rm A}$ quenching.

DOI:10.5506/APhysPolB.49.237

1. Introduction

The issue of the quenching of $g_{\rm A}$ in the context of neutrinoless double beta ($0\nu\beta\beta$) decay has recently surfaced [1]. The related decay rates are affected by the available phase space (Q values), the nuclear matrix elements (NMEs) and the value of $g_{\rm A}$ in its fourth power [2–5]. The $0\nu\beta\beta$ decay relates to Majorana neutrinos and their mass scale, as also to the breaking of the lepton-number symmetry and to the baryon asymmetry of the Universe [6]. A number of nuclear models, including configuration-interaction-based models such as the interacting shell model (ISM) and the proton–neutron quasiparticle random-phase approximation (pnQRPA), and various mean field models have been adopted for the calculations. The resulting computed NMEs have been analyzed in the review articles [5, 7, 8].

A lot of attention has been paid to the calculation of the NMEs related to the $0\nu\beta\beta$ decay. Less attention has been paid, at least in the theory community, to the possible (large) quenching of $g_{\rm A}$ and its possibly disastrous impact on the sensitivities of the present and planned $0\nu\beta\beta$-decay experiments [1]. This deviation (usually quenching) from the free-nucleon value

* Presented at the XXXV Mazurian Lakes Conference on Physics, Piaski, Poland, September 3–9, 2017.

$g_{\rm A} = 1.27$ can arise from the *nuclear medium effects* and the *nuclear many-body effects*. The former contain quenching related to the presence of spin-multipole giant resonances [9], non-nucleonic degrees of freedom (like the Δ isobar [10, 11]) and meson-exchange-driven two-body weak currents [12–14]. The latter relates to deficiencies of the nuclear many-body approaches used to compute the wave functions involved in the decay transitions. This means that the effective values of $g_{\rm A}$ can vary from one nuclear model to the other. The renormalization of $g_{\rm A}$ can also depend on the process in question. For the zero-momentum-exchange processes, like β decays, the renormalization can be different from the high-momentum-exchange (~ 100 MeV) processes, like $0\nu\beta\beta$ decays.

The effective value of $g_{\rm A}$ relates to the *renormalization factor* q (in the case of quenching, it is called *quenching factor*)

$$q = \frac{g_{\rm A}}{g_{\rm A}^{\rm free}}\,, \tag{1}$$

where

$$g_{\rm A}^{\rm free} = 1.2723(23) \tag{2}$$

is the free-nucleon value of the axial-vector coupling measured in neutron beta decay [15] and $g_{\rm A}$ is the value of the axial-vector coupling derived from a given theoretical or experimental analysis. This derived $g_{\rm A}$ can be called the *effective* $g_{\rm A}$ so that from (1) one obtains for its value

$$g_{\rm A}^{\rm eff} = q g_{\rm A}^{\rm free}\,. \tag{3}$$

This effective value of $g_{\rm A}$ for β decays will be studied below in several different contexts.

2. Quenching of $g_{\rm A}$ in Gamow–Teller β decays

Gamow–Teller decays are mediated by the Pauli spin operator $\boldsymbol{\sigma}$ [16] and they thus change the initial nuclear spin $J_{\rm i}$ by one unit. In the renormalization studies, the simplest Gamow–Teller transitions are selected, namely the ground-state-to-ground-state ones. Traditionally, the renormalization of the axial-vector coupling strength has been studied in the framework of the interacting shell model (ISM) in a number of calculations of the Gamow–Teller β decays of very light (p-shell), light (sd-shell), and medium-heavy (pf-shell and sdg-shell) nuclei. In these calculations, it appears that the value of $g_{\rm A}$ is quenched. As indicated by the ISM results collected in Table I and depicted in Fig. 1, the quenching factor (1) is roughly a decreasing function of the nuclear mass number A, implying stronger quenching with increasing nuclear mass.

TABLE I

Mass ranges and effective values of g_A extracted from the works of the last column.

Mass range	g_A^{eff}	Reference
Full $0p$ shell	$1.03^{+0.03}_{-0.02}$	[17]
$0p$–low $1s0d$ shell	1.18 ± 0.05	[18]
Full $1s0d$ shell	$0.96^{+0.03}_{-0.02}$	[19] (see also [20])
	1.0	[21]
$A = 41$–50 ($1p0f$ shell)	$0.937^{+0.019}_{-0.018}$	[22] (see also [20])
$1p0f$ shell	0.98	[21]
^{56}Ni	0.71	[21]
$A = 52$–67 ($1p0f$ shell)	$0.838^{+0.021}_{-0.020}$	[23]
$A = 67$–80 ($0f_{5/2}1p0g_{9/2}$ shell)	0.869 ± 0.019	[23]
$A = 63$–96 ($1p0f0g1d2s$ shell)	0.8	[24]
$A = 76$–82 ($1p0f0g_{9/2}$ shell)	0.76	[25]
$A = 90$–97 ($1p0f0g1d2s$ shell)	0.60	[26]
^{100}Sn	0.52	[21]
$A = 128$–130 ($0g_{7/2}1d2s0h_{11/2}$ shell)	0.72	[25]
$A = 130$–136 ($0g_{7/2}1d2s0h_{11/2}$ shell)	0.94	[27]
$A = 136$ ($0g_{7/2}1d2s0h_{11/2}$ shell)	0.57	[25]

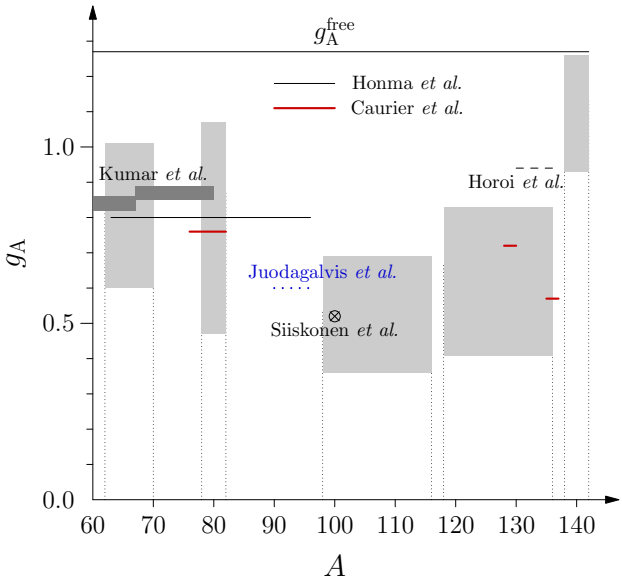

Fig. 1. Ranges of averaged effective values of g_A from the pnQRPA calculations (light-hatched regions) plotted against the ISM results of Table I. The ISM results come from [24] (Honma *et al.*), [25] (Caurier *et al.*), [26] (Juodagalvis *et al.*), [23] (Kumar *et al.*, dark-hatched regions), and [21] (Siiskonen *et al.*).

In Fig. 1, the ISM results are contrasted against those obtained by the use of the proton–neutron quasiparticle random-phase approximation (pnQRPA) in [28–30] (see also [31]). The pnQRPA results constitute the light-hatched regions in the background of the ISM results. The hatched regions are indicative of the effect of the leading proton–neutron configurations that change from one region to the other. For example, a displacement is seen between $A = 70$–78 where the dominating proton–neutron configuration of the nuclear wave functions shifts from the $1p$ orbitals to the $0g$ orbitals. As can be seen in the figure, the ISM results and the pnQRPA results are in surprisingly good agreement with each other, considering the quite different bases of these two different many-body frameworks.

3. Quenching of g_{A} in forbidden unique β decays

The forbidden unique β transitions are the simplest ones that mediate β decays between nuclear states with angular-momentum difference ΔJ larger than 1. In particular, if one of the states is a 0^+ state, then for a K^{th} forbidden ($K = 1, 2, 3, \ldots$) unique beta decay, the angular momentum of the other involved state is $J = K + 1$. At the same time, the parity changes in the odd-forbidden and remains the same in the even-forbidden decays [16]. The change in angular momentum and parity for different degrees of forbiddenness of the unique transitions obeys the simple rule

$$(-1)^{\Delta J}\pi_{\mathrm{i}}\pi_{\mathrm{f}} = -1\,. \tag{4}$$

In fact, also the Gamow–Teller decays obey rule (4) if one of the involved nuclear states has the multipolarity 0^+.

The forbidden unique beta transitions relate to the possible quenching of these intermediate multipole transitions in the GT-type of $0\nu\beta\beta$ NME. In a simplistic approach, this quenching can be condensed into an effective axial coupling, $g^{\mathrm{eff}}_{\mathrm{A},0\nu}$, multiplying the $0\nu\beta\beta$ GT-type of NME

$$M^{(0\nu)}_{\mathrm{GTGT}} = \left(g^{\mathrm{eff}}_{\mathrm{A},0\nu}\right)^2 \sum_{J^\pi} \left(0^+_{\mathrm{f}}||\mathcal{O}^{(0\nu)}_{\mathrm{GTGT}}(J^\pi)||0^+_{\mathrm{i}}\right)\,, \tag{5}$$

where $\mathcal{O}^{(0\nu)}_{\mathrm{GTGT}}$ denotes the transition operator mediating the $0\nu\beta\beta$ transition through the various multipole states J^π, 0^+_{i} denotes the initial ground state, and the final ground state is denoted by 0^+_{f}. The effective axial coupling relevant for $0\nu\beta\beta$ decay is denoted as $g^{\mathrm{eff}}_{\mathrm{A},0\nu}$ to emphasize that its value may deviate from the one determined in single β and $2\nu\beta\beta$ decays. The virtual transitions corresponding to the $A = 116$ case are depicted in Fig. 2.

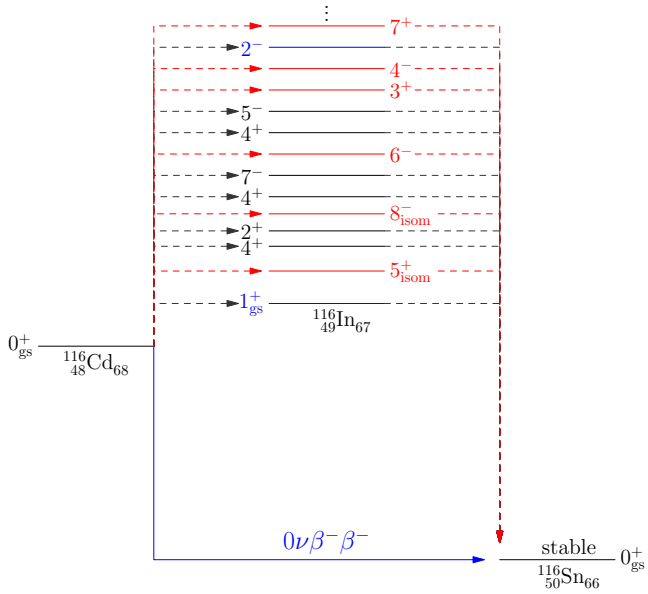

Fig. 2. The $0\nu\beta\beta$ decay of ^{116}Cd to ^{116}Sn via the virtual intermediate states in ^{116}In. The transitions between ^{116}Cd (^{116}Sn) and ^{116}In constitute the left-leg (right-leg) transitions.

The remarkable feature of Eq. (5) is that the effective axial coupling strength is raised to 2$^{\text{nd}}$ power making the value of $g^{\text{eff}}_{\text{A},0\nu}$ play an extremely important role in determining the $0\nu\beta\beta$-decay rate which is (neglecting the smaller double Fermi and tensor contributions) proportional to the squared NME and thus to the 4$^{\text{th}}$ power of the coupling

$$0\nu\beta\beta - \text{rate} \sim \left|M^{(0\nu)}_{\text{GTGT}}\right|^2 = g^4_{\text{A},0\nu}\left|\sum_{J^\pi}\left(0^+_{\text{f}}||\mathcal{O}^{(0\nu)}_{\text{GTGT}}(J^\pi)||0^+_{\text{i}}\right)\right|^2 . \qquad (6)$$

3.1. First-forbidden unique β decays

The first-forbidden unique β transitions are mediated by a rank-2 (*i.e.* having angular-momentum content 2) parity-changing spherical tensor operator. In the quenching studies, it is advantageous to use the simplest first-forbidden transitions, namely the ground-state-to-ground-state ones. In Fig. 3, there are depicted the first-forbidden unique ground-state-to-ground-state β^- and β^+/EC transitions between even–even 0^+ and odd–odd 2^- ground states in the $A = 84$ Ge–As–Se and $A = 82$ Se–Br–Kr isobaric chains. Shown is the lateral feeding from a middle odd–odd nucleus to adjacent even–even ground states. In the figure, the transition NME is denoted by M_{L} (M_{R}) in the case it is to the left (right) of the central nucleus.

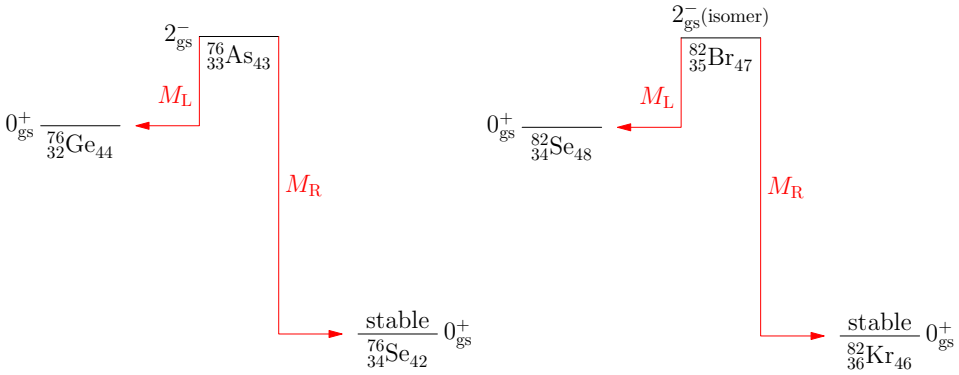

Fig. 3. First-forbidden unique beta decays in the $A = 76$ Ge–As–Se and $A = 82$ Se–Br–Kr isobaric chains.

In [32], 19 first-forbidden unique ground-state-to-ground-state β-decay transitions were studied. The interesting transitions are the ones where both $M_{\rm L}$ and $M_{\rm R}$ NMEs are known experimentally. In this case, one can use the geometric mean

$$\bar{M}_{\rm GT} = \sqrt{M_{\rm L} M_{\rm R}} \tag{7}$$

of the left and right NMEs in the analysis, making the analysis more stable. The obtained values in [32] were

$$g_{\rm A}^{\rm eff} \approx 0.57 \tag{8}$$

for the effective axial-vector coupling strength using the pnQRPA wave functions. The average of the values of the leading two-quasiparticle NMEs gives in turn

$$g_{\rm A}^{\rm eff}(\text{2qp}) \approx 0.23\,, \tag{9}$$

implying the ratio

$$k = \frac{\bar{M}_{\rm pnQRPA}}{\bar{M}_{\rm qp}} = 0.4 \tag{10}$$

and thus a drastic nuclear many-body effect when going from the two-quasiparticle level of approximation to the pnQRPA level. The 2qp-NME to pnQRPA-NME comparison offers a clean separation between the nuclear-medium effects and the nuclear-model effects, the nuclear-model effect being responsible for the (in this case large) shift in the values of the NMEs.

4. Higher-forbidden unique β decays

The $0\nu\beta\beta$ decays proceed via virtual intermediate states of all multipolarities J^π due to the multipole expansion of the Majorana-neutrino propagator (see, *e.g.*, [2, 4, 33–38]). In [39], 148 potentially measurable second-,

third-, fourth-, fifth-, sixth- and seventh-forbidden unique beta transitions were studied. The aim of the work [39] was to shed light on the magnitudes of the NMEs corresponding to the high-forbidden unique $0^+ \leftrightarrow J^\pi = 3^+, 4^-, 5^+, 6^-, 7^+, 8^-$ virtual transitions taking part in neutrinoless double beta decay, as shown in Fig. 2.

In [39], the ratio k of the NMEs, calculated by the pnQRPA, M_{pnQRPA}, and a two-quasiparticle model, M_{qp}, was studied and compared with earlier calculations for the allowed Gamow–Teller 1^+ [28] and first-forbidden spin–dipole (SD) 2^- [32] transitions. Based on this comparison, the *expected* half-lives of the studied β-decay transitions were obtained, one example being the expected half-lives of fourth- and seventh-forbidden β decays shown in Fig. 4.

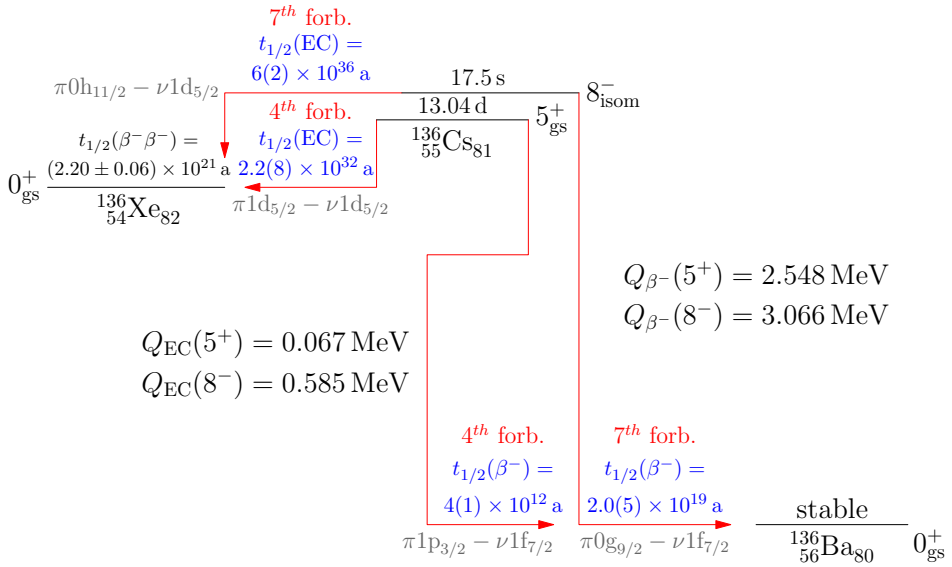

Fig. 4. Predicted half-lives and their error estimates (in parentheses) for β^- and EC (electron-capture) transitions in the isobaric chain $A = 136$. The spin-parity assignments, decay energies (Q values) and life-times of the nuclear ground (gs) and isomeric (isom) states are experimental data and taken from [40]. The $2\nu\beta\beta$ half-life is taken from [41]. In addition to the half-lives, the degree of forbiddenness and the leading single-particle transition are shown.

Based on the analysis of [39], the ratio k is, in the gross, independent of the degree of forbiddenness and thus the (low-energy) forbidden unique contributions [obeying the simple rule (4)] to the $0\nu\beta\beta$ NME (6) should be roughly uniformly quenched. If these conclusions can be generalized to

include also the non-unique β transitions, obeying the rule

$$(-1)^{\Delta J}\pi_{\rm i}\pi_{\rm f} = +1\,, \tag{11}$$

one can then speak about an effective axial coupling, $g_{\rm A,0\nu}^{\rm eff}$, in front of the $0\nu\beta\beta$ NME in (5), at least for "low" excitation energy in the intermediate nucleus, "low" being still an undefined notion that has to be investigated in future works.

5. Quenching of $g_{\rm A}$ in forbidden non-unique β decays

The shape functions of forbidden non-unique beta decays are complicated combinations of different NMEs and phase-space factors. Furthermore, their dependence on the weak coupling strengths $g_{\rm V}$ (vector part) and $g_{\rm A}$ (axial-vector part) is very non-trivial. In fact, the shape factor $C(w_e)$ can be decomposed into vector, axial-vector and mixed vector-axial-vector parts in the form of [42]

$$C(w_e) = g_{\rm V}^2 C_{\rm V}(w_e) + g_{\rm A}^2 C_{\rm A}(w_e) + g_{\rm V}g_{\rm A}C_{\rm VA}(w_e)\,. \tag{12}$$

In [42], it was proposed that the shapes of β-electron spectra could be used to determine the values of the weak coupling strengths by comparing the computed spectrum with the measured one for forbidden non-unique β decays. This method was coined the spectrum-shape method (SSM). In this study, also the next-to-leading-order corrections to the β-decay shape factor were included. In [42], the β-electron spectra were studied for the $4^{\rm th}$-forbidden non-unique ground-state-to-ground-state β^- decay branches $^{113}{\rm Cd}(1/2^+) \to {}^{113}{\rm In}(9/2^+)$ and $^{115}{\rm In}(9/2^+) \to {}^{115}{\rm Sn}(1/2^+)$ using the microscopic quasiparticle-phonon model (MQPM) [43] and the ISM.

The work of [42] was extended in [44] to include an analysis made by using a third nuclear model, the microscopic interacting boson–fermion model (IBFM-2) [45]. It was noticed that the β spectrum shapes of both transitions are highly sensitive to the values of $g_{\rm V}$ and $g_{\rm A}$, and hence comparison of the calculated spectrum shape with the measured one opens a way to determine the values of these coupling strengths. As a by-product, it was found that for all values of $g_{\rm A}$, the best fits to data were obtained by using the canonical value $g_{\rm V} = 1.0$ for the vector coupling strength. A striking feature of the SSM analysis was that the three models yield a consistent result, $g_{\rm A} \approx 0.92$, when the SSM is applied to the available experimental β spectrum [46] of ^{113}Cd. The result is illustrated in Fig. 5, where the three curves overlap best at the values $g_{\rm A}^{\rm eff} = 0.92$ (MQPM), $g_{\rm A}^{\rm eff} = 0.90$ (ISM), and $g_{\rm A}^{\rm eff} = 0.93$ (IBFM-2).

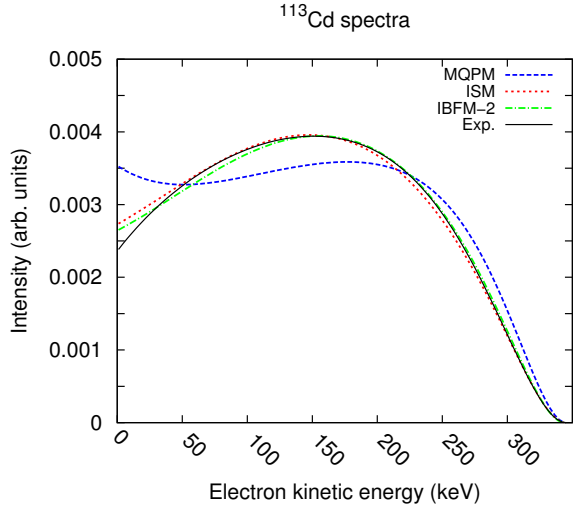

Fig. 5. Comparison of the computed β spectra of ^{113}Cd with the experiment. The next-to-leading-order corrections to the shape factor have been included, and only the best matches are shown in the figure. The canonical value $g_{\rm V} = 1.0$ is used for the vector coupling strength. The areas under the curves are normalized to unity.

The works [42, 44] were continued by the works [47] and [48], where the evolution of the β spectra with changing value of $g_{\rm A}$ was followed for a number of highly-forbidden β^- decays of odd-A nuclei (MQPM and ISM calculations) and even-A nuclei (ISM calculations). In Fig. 6, a comparison of the MQPM (left panel) and ISM (right panel) calculations [48] for the β spectrum of the second-forbidden non-unique decay transition ^{99}Tc$(9/2^+) \rightarrow {}^{99}Ru(5/2^+)$ is shown. There is clear sensitivity to the value of $g_{\rm A}$. Remarkably, the spectrum shapes computed by the two nuclear mod-

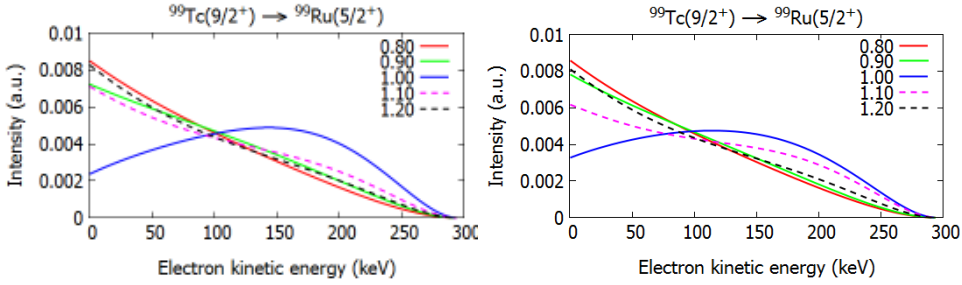

Fig. 6. (Color online) Normalized electron spectra for the second-forbidden non-unique ground-state-to-ground-state β^- decay of ^{99}Tc as computed by using the MQPM (left panel) and the ISM (right panel). The value $g_{\rm V} = 1.0$ was assumed and the color coding represents the value of $g_{\rm A}$.

els agree almost perfectly, giving evidence in favor of the robustness of the SSM. Experimentally, the branching to this decay channel is practically 100% so that the β spectrum is potentially well measurable.

6. Conclusions

The issue of $g_{\rm A}$ renormalization is far from being solved and lacks a unified picture thus far. There is not yet a coherent effort to solve the issue, but rather some scattered attempts here and there. The most critical issue may be the nuclear many-body deficiencies that hinder a quantitative assessment of the nuclear-medium effects in light, medium-heavy and heavy nuclei. Only gradually this state of affairs will improve with the progress in the *ab initio* nuclear methods extendable to nuclei beyond the very lightest ones. The hope is that in the future the different studies would point to one common low-energy renormalization of $g_{\rm A}$ for the β decays and that we would have some idea about the renormalization mechanisms at work in the case of the neutrinoless $\beta\beta$ decays.

In a promising new method, the spectrum-shape method, the comparison of the computed and measured β spectra of high-forbidden non-unique β decays is exploited. The robustness of the method is based on the observations that the computed spectra seem to be relatively insensitive to the adopted mean-field and nuclear models. Measurements of such electron spectra for certain key transitions are encouraged. Also the relation of the quenching of the Gamow–Teller strength and forbidden unique β transitions is pointed out.

This work was supported by the Academy of Finland under the Finnish Center of Excellence Program 2012–2017 (Nuclear and Accelerator Based Program at JYFL)

REFERENCES

[1] J. Suhonen, *Phys. Rev. C* **96**, 055501 (2017) [arXiv:1708.09604 [nucl-th]].

[2] J. Suhonen, O. Civitarese, *Phys. Rep.* **300**, 123 (1998).

[3] J. Maalampi, J. Suhonen, *Adv. High Energy Phys.* **2013**, 505874 (2013).

[4] J.D. Vergados, H. Ejiri, F. Šimkovic, *Int. J. Mod. Phys. E* **25**, 1630007 (2016).

[5] J. Engel, J. Menéndez, *Rep. Prog. Phys.* **80**, 046301 (2017).

[6] F.F. Deppisch *et al.*, *Phys. Rev. D* **92**, 036005 (2015).

[7] J. Suhonen, O. Civitarese, *J. Phys. G: Nucl. Part. Phys.* **39**, 085105 (2012).

[8] J. Suhonen, O. Civitarese, *J. Phys. G: Nucl. Part. Phys.* **39**, 124005 (2012).
[9] L. Jokiniemi, J. Suhonen, *Phys. Rev. C* **96**, 034308 (2017).
[10] E. Oset, M. Rho, *Phys. Rev. Lett.* **42**, 47 (1979).
[11] A. Bohr, B.R. Mottelson, *Phys. Lett. B* **100**, 10 (1981).
[12] L.S. Towner, *Phys. Rep.* **155**, 263 (1997).
[13] J. Menéndez, D. Gazit, A. Schwenk, *Phys. Rev. Lett.* **107**, 062501 (2011).
[14] A. Ekström *et al.*, *Phys. Rev. Lett.* **113**, 262504 (2014).
[15] C. Patrignani *et al.* [Particle Data Group], *Chin. Phys. C* **40**, 100001 (2016).
[16] J. Suhonen, *From Nucleons to Nucleus: Concepts of Microscopic Nuclear Theory*, Springer, Berlin 2007.
[17] W.T. Chou, E.K. Warburton, B.A. Brown, *Phys. Rev. C* **47**, 163 (1993).
[18] D.H. Wilkinson, *Nucl. Phys. A* **225**, 365 (1974).
[19] B.H. Wildenthal, M.S. Curtin, B.A. Brown, *Phys. Rev. C* **28**, 1343 (1983).
[20] M. Konieczka, P. Bączyk, W. Satuła, *Phys. Rev. C* **93**, 042501(R) (2016).
[21] T. Siiskonen, M. Hjorth-Jensen, J. Suhonen, *Phys. Rev. C* **63**, 055501 (2001).
[22] G. Martínez-Pinedo, A. Poves, E. Caurier, A.P. Zuker, *Phys. Rev. C* **53**, R2602 (1996).
[23] V. Kumar, P.C. Srivastava, H. Li, *J. Phys. G: Nucl. Part. Phys.* **43**, 105104 (2016).
[24] M. Honma, T. Otsuka, T. Misuzaki, M. Hjorth-Jensen, *J. Phys.: Conf. Ser.* **49**, 45 (2006).
[25] E. Caurier, F. Nowacki, A. Poves, *Phys. Lett. B* **711**, 62 (2012).
[26] A. Juodagalvis, D.J. Dean, *Phys. Rev. C* **72**, 024306 (2005).
[27] M. Horoi, A. Neacsu, *Phys. Rev. C* **93**, 024308 (2016).
[28] H. Ejiri, J. Suhonen, *J. Phys. G: Nucl. Part. Phys.* **42**, 055201 (2015).
[29] P. Pirinen, J. Suhonen, *Phys. Rev. C* **91**, 054309 (2015).
[30] F.F. Deppisch, J. Suhonen, *Phys. Rev. C* **94**, 055501 (2016).
[31] D.S. Delion, J. Suhonen, *Europhys. Lett.* **107**, 52001 (2014).
[32] H. Ejiri, N. Soukouti, J. Suhonen, *Phys. Lett. B* **729**, 27 (2014).
[33] M. Kortelainen, O. Civitarese, J. Suhonen, J. Toivanen, *Phys. Lett. B* **647**, 128 (2007).
[34] M. Kortelainen, J. Suhonen, *Phys. Rev. C* **75**, 051303(R) (2007).
[35] M. Kortelainen, J. Suhonen, *Phys. Rev. C* **76**, 024315 (2007).
[36] J. Suhonen, M. Kortelainen, *Int. J. Mod. Phys. E* **17**, 1 (2008).
[37] J. Hyvärinen, J. Suhonen, *Phys. Rev. C* **91**, 024613 (2015).
[38] J. Hyvärinen, J. Suhonen, *Adv. High Energy Phys.* **2016**, 4714829 (2016).
[39] J Kostensalo, J. Suhonen, *Phys. Rev. C* **95**, 014322 (2017).
[40] ENSDF at NNDC site, `http://www.nndc.bnl.gov/`

[41] A.S. Barabash, *AIP Conf. Proc.* **1572**, 11 (2013) [arXiv:1311.2421 [nucl-ex]].
[42] M. Haaranen, P.C. Srivastava, J. Suhonen, *Phys. Rev. C* **93**, 034308 (2016).
[43] J. Toivanen, J. Suhonen, *Phys. Rev. C* **57**, 1237 (1998).
[44] M. Haaranen, J. Kotila, J. Suhonen, *Phys. Rev. C* **95**, 024327 (2017).
[45] F. Iachello, P. Van Isacker, *The Interacting Boson–Fermion Model*, Cambridge University Press, Cambridge USA, 1991.
[46] P. Belli *et al.*, *Phys. Rev. C* **76**, 064603 (2007).
[47] J. Kostensalo, M. Haaranen, J. Suhonen, *Phys. Rev. C* **95**, 044313 (2017).
[48] J. Kostensalo, J. Suhonen, *Phys. Rev. C* **96**, 024317 (2017).